Journal of Engineering and Sustainable Development
http://jeasd.uomustansiriyah.edu.iq
https://doi.org/10.31272/jeasd.25.1.10

JEASD

Vol. 25, No. 01, January 2021
ISSN 2520-0917

THERMAL PERFORMANCE ENHANCEMENT OF A VERTICAL THERMOSYPHON HEAT PIPE BY FLOW CONTROL OF THE TWO PHASES

***Alaa A. B. Temimy[1]** **Adnan A. Abdulrasool[2]**

1) Training and Power Research Office, Ministry of Electricity, Baghdad, Iraq
2) Mechanical Engineering Department, Mustansiriayah University, Baghdad, Iraq

Received 5/1/2020 ***Accepted in revised form 19/7/2020*** ***Published 1/1/2021***

Abstract: Heat Pipe (THP) has a continues evaporation/ condensation cycles of the working fluid. The flow patterns of the two phases is founds by previous published articles, as a non-steady complex spatial flow pattern. This type of the flow blocks the easy moving of the two-phases and limits the thermal performance of the THP. In this study, a copper tubes packing (TP) is simulated numerically to control/manage the flow streams of the two phases inside the THP. The simulated THP is 600mm length made of copper partially filled with water. The TP is consist of a two copper tubes attached contrary to each other with a neighboring openings. The upper tube (Riser tube) facilitate the moving of steam streams from evaporator section to the top of the condenser section. The lower tube (Down-comer tube) facilitate the moving of the condensate streams from the condenser section to the bottom of the evaporator section. The tested filling ratios are (40,50,55,60 and 70) % of evaporator section volume. The supplied heats are (50,75,100,150 and 200) W. The Computational Fluid Dynamics solution are done for a three dimensional model (3DCFD) using ANSYS/ Fluent R19.0 software. The simulation result of the steam volume fractions contours shows that the insertion of TP control the flow streams of both phases. Also prevent the formation of complex flow patterns then enhance the axial velocity vectors and reduce cross velocity vectors. The inserted TP provide a regular circulation paths for the working fluid phases and enhance evaporation /condensation processes. Hence it's reduce the thermal resistance of the THP about 55% and enhance the thermal performance with the same percentage. In addition, the thermal performance of the enhanced TPTHP is not/a little influence due to the variation of the filling ratio.

Keywords: *Two-phase thermosyphone, Wickless, Heat pipe, performance, Computational fluid dynamics (CFD), Flow pattern modelling, Evaporation, Condensation, Water*

1. Introduction

Two phase Closed Heat Pipe (THP) is considered as one of the power-full devices in heat transfer and heat homogeneity [1]. That because its high capabilities for heat transfer without external source of power, i.e. passive heat transfer device [2]. The THP divided based on the working principles into a three sections [3]: evaporator section, adiabatic section and condenser section. A continues cycles of evaporation and condensation processes presents the THP working principles. A schematic diagram for the THP sections and working principles is shown in Fig.(1) [4]. Due to its low manufacturing cost, wide range of working fluids and materials, no-maintenance requirements and simplicity, the THPs are used in a very wide range of applications. Some of these applications are solar applications [5], [6] , cooling of electronics [7][8], air conditioning applications [9] , satellites and space applications [10], [11]. Therefore, improving/enhancement the thermal performance of the THP is a demand for many

**Corresponding Author*: dralaatemimy@yahoo.com

researchers and application producers for a cooling devices with high rates of heat transfer.

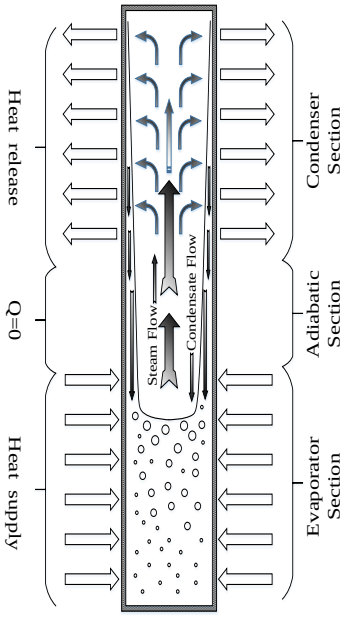

Figure 1. Schematic Diagram of THP Longitudinal Section and Operation Principles [4]

The enhancement techniques used for increasing the thermal performance of the THP can be categorized in four categories. (a) Using of nano fluids to enhance the thermal performance of the working fluid as tested by M. Rahimi et.al. [12], T. Israeli et.al , 2008 [13] , S. Zhao et.al , 2018 [14]…etc... (b) Using of binary mixtures of fluid as working fluid with relatively high rates of wettability or self-rewetting fluids as tested by K. Armijo et.al , 2011 [15] , Y. Naresh et.al. , 2018 [16] … etc..(c) Using of phase change materials (PCM) to control the temperatures fluctuations of the THP during transient and steady state operations as tested by Y. Weng et.al , 2011 [17], H. Behi et.al. , 2017 [18]… etc..(d) Geometry modification techniques. This technique focused on the THP geometrical aspects to enhance the thermal performance of the THP as proposed and tested by the following authors. H. Hashimoto et.al , 2002 [19] , studied experimentally the effect of entrainment on heat transfer drop in the condenser of THP. They tested the effects of the variation of evaporator section diameter on the reduction of entrainments in the evaporator section. Two test rigs are constructed and tested with water, ethanol, and R113 as working fluids. The evaporator is made of copper with same ID/OD of condenser section for test rig #1. While a stainless steel 304 tube with larger ID was used as evaporator section for test rig #2. The authors reported that the effect of entrainment on the condenser thermal performance can't confirmed in their study. But the temperature distribution along the evaporator section of test rig #2 has a better performance than that of test rig #1. Y. Hung et.al. , 2011 [20] , developed 1D mathematical model to study the effect of some geometrical parameters on heat transfer capacity of THP. These geometrical parameters are star grooves, cross sectional area, length, adiabatic section length and FR. The star grooves types are: triangle, square, hexagonal, and octagonal. They concluded that for a thin grooves the heat transfer capacity increases due to the increase of capillary forces. Also they showed that heat transfer capacity is proportional to the cross sectional area and inversely to the length of THP. Hence heat transfer increases when adiabatic section length decreases at constant THP total length. R. Nair et.al , 2016 [21], studied numerically the effects of the insertion of a rectangular longitudinal fins (along condenser section). Also studied the effects of the number of fins on enhancement of thermal performance (condensate mass) of THP at steady state conditions. The fins are inserted and attached to the inner surface of the condenser section to increase the effective area of condensation. The results showed that the condensate mass increase about 22% for 8 fins, and about 32% for 12 fins. A. B. Solomon et.al , 2017 [22], studied the THP thermal performance with/without a thin porous copper coat at the inner surface of a coper pipe. The thin layer of porous copper was established

to enhance pool boiling process. This layer was made using electrochemical deposition process. Also they tested the effects of coating with oxides on the thermal performance. They found that the copper coat showed a better heat transfer capabilities better than oxide coat and the un-coated pipe. Thermal resistance (R_{th}) was lowered about 21% at inclination angle of 45º and 10 kW/m^2 heat flux. S. Fertahi et.al. , 2018 [23] , set up a 2D CFD numerical simulation to simulate THP operation for domestic water heating system. The authors showed that the results were validated with a previous published work and a good agreement were achieved. Also they suggested that the insertion of tilted fins at condenser section will enhance the thermal performance of THP. A. Alammar et.al. , 2018 [24] , studied experimentally the effect of roughness of the internal surface on thermal performance of THP. The roughness is made with electrical discharging machine for the copper. The surface roughness reduces R_{th} about 16%. Y. Kim et.al. , 2019 [25] , tested experimentally the effect of sintered microporous coating of evaporator section on THP thermal performance. The results showed that reduction in R_{th} about 51% at FR 35% and about 30% at FR 70%. A. Temimy et.al. , 2019 [4], simulate numerically the flow patterns of the working fluid inside the THP. The simulation results showed that the flow patterns are not as ordinary assumed, where the steam flow upward at the core and the condensate flow at the inner surface of the THP. The simulation showed that the flow patterns are a complex flow behavior. Also a non-steady spatial flow occurring for both phases as shown in fig. (2) for velocity vectors. The velocity vectors showed that non-steady and non-stable vortices fields are formed. Also the axial flow velocity vectors (along the THP) in upward/downward directions are not clear. Cross velocity vectors are clear at different elevations. The axial flow velocity vectors, are the responsible vectors for heat/mass transfer along the THP. While cross velocity vectors are responsible for complex/vortex flow formation. The temperatures distribution along the THP are validated by experimental tests for the same working configurations by the authors in 2019 [26].

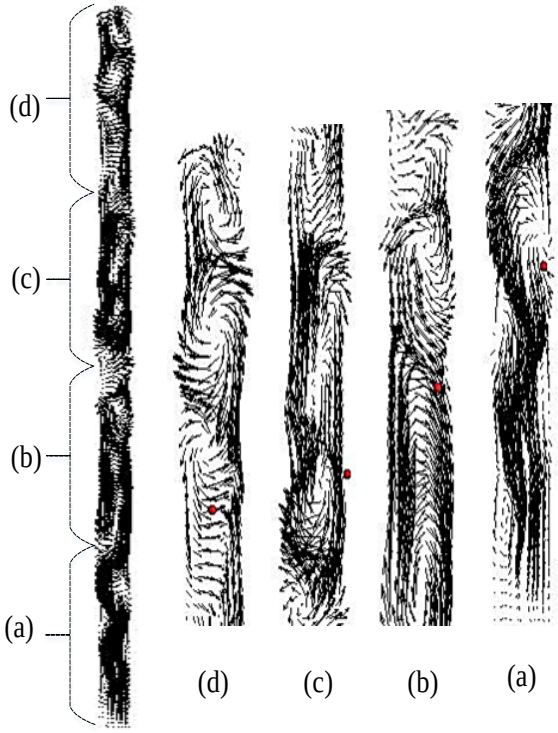

Figure 2. Velocity Vectors at Vertical Central Section of THP [4]

As described above, the THP thermal performance enhancement techniques focused on the thermal properties of the THP material and working fluid and the area heat transfer. Studies on the effect of the flow patterns behavior inside the THP on the thermal performance is rare. In this study, the suggested goals are to design and simulate numerically the effect of an insertion a new tubes packing (TP) on the two-phases flow patterns. This TP consist of a two copper tubes attached contrary to each other with a neighboring openings. The upper tube (Riser tube) is proposed to facilitate the moving of steam streams from evaporator section to the top

of the condenser section. The lower tube (Down-comer tube) is proposed to facilitate the moving of the condensate streams from the condenser section to the bottom of the evaporator section. Therefore, the insertion of this TP into the THP will separate the flow paths/streams of both phases. Hence, it will provide a uniform circulation cycle for the working fluid and prevent formation of complex spatial flow patterns. The proposed uniform circulation cycle for the working fluid will enhance evaporation and condensation processes and leads to enhance the thermal performance of the THP.

2. Model Geometry and Dimensions

The modeled THP is made from copper pipe has OD/ID of 19.05mm/ 17.4mm with 600mm length. The length is divided as 250mm as evaporator section, 150mm as adiabatic section and 200mm as condenser section as shown in fig. (3). The condenser section cooled by a jacketed heat exchanger along the condenser with OD of 50mm with cooling water flowrate of 3 lit./min.. The supplied heat set as a constant heat flux at the evaporator section surface with values of (50, 75, 100, 150, 200) W. Filling ratios (FR) are (40, 50, 55, 60, 70) % of the evaporator volume.

The proposed two phases flow paths controller Tubes Packing (TP) consist of two copper tubes assigned as riser tube and down comer tube. The riser tube controls the flow paths of the steam streams. The generated steam guided upward by the buoyancy forces to the top of the condenser section without any interactions with the condensate streams. The down comer tube controls the flow paths of the condensate streams. The condensate guided downward by the gravitational forces to the bottom of the evaporator section without any interactions with the steam streams as shown in fig. (4) for the TPTHP.

The TP tubes arranged in a parallel position with a 10mm shifting in their openings. The riser tube has a length of 305mm and OD/ID of 9.5mm / 8.3mm. The down comer tube has a length of 230mm and OD/ID of 6.2mm / 5mm. The tubes are connected to central disk of thickness 10mm and OD of 15.8mm. The central disk allocated at a level of 250mm from the bottom of the THP. Therefore, the upper opening of the riser tube will be at a level of 550mm, and the lower opening of the down comer tube will be at a level of 25mm as shown in fig. (5).

Mesh independency procedure are used and the final mesh of about 4.5M nodes are set as shown in fig. (6). The transient solution time step independency procedures are used and a time step of 10^{-4} Sec. This time step provide a Courant Number less than unity [4], [26].

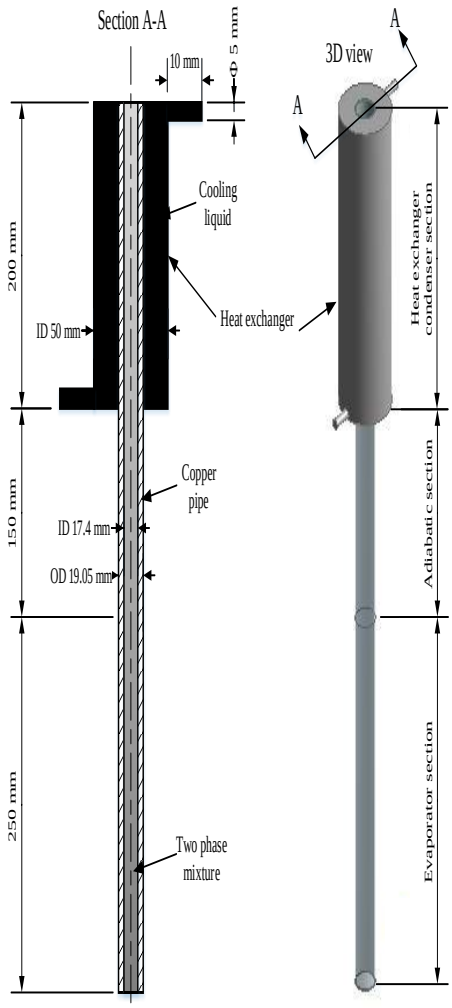

Figure 3. THP Model Geometry and Dimensions

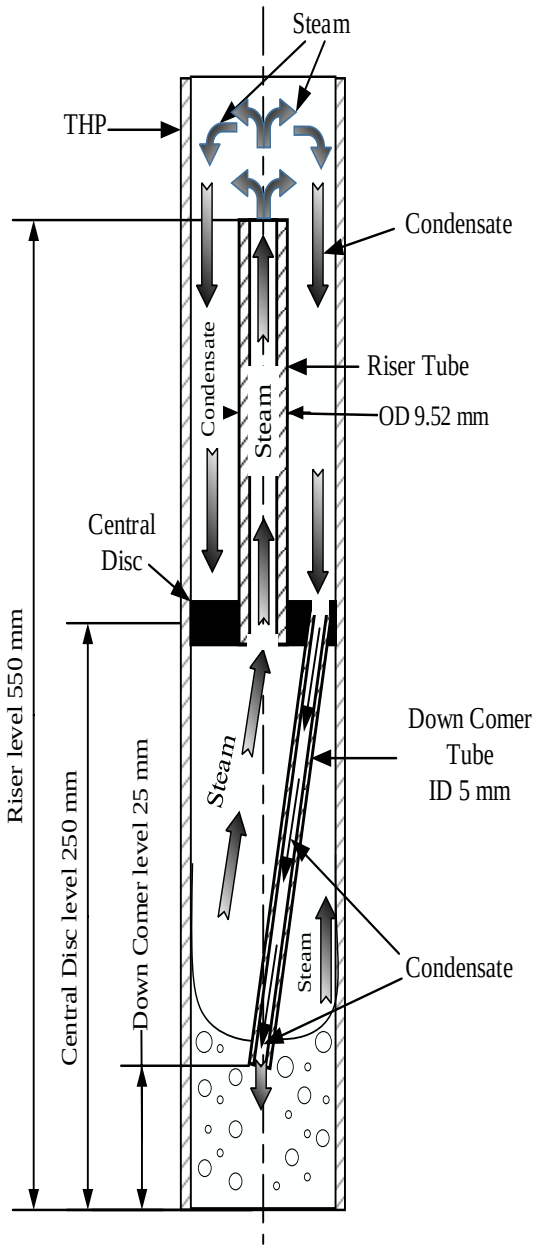

Figure 4. TPTHP Schematic Diagram and Dimensions

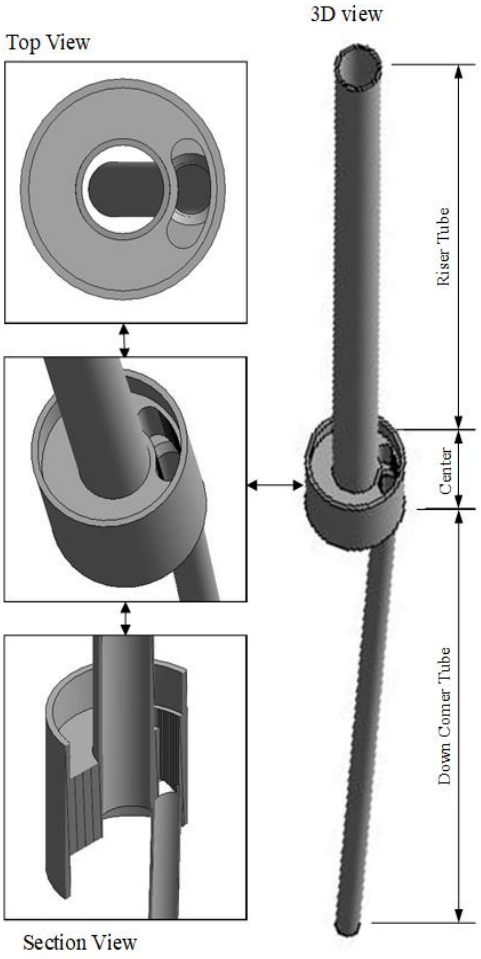

Figure 5. Tubes Packing Model and Geometry

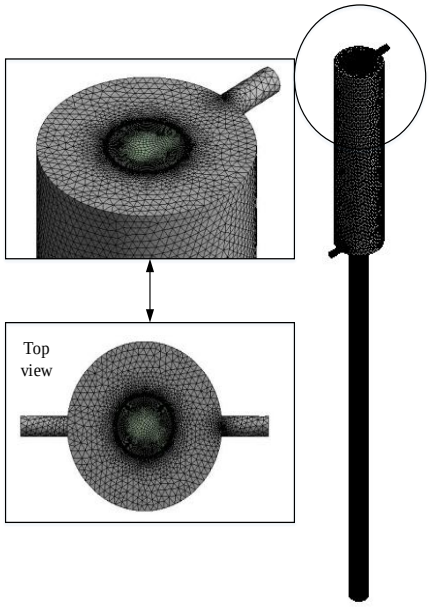

Figure 6. 3D CFD Model Mesh, about 4.5M Million nodes

3. Governing Equations

The case study includes fluid flow, heat transfer and mass transfer between two-phases of single fluid (steam and condensate of water). Therefore, one of the available Euler-Euler solution models in Fluent was selected which is the Volume Of Fluid model (VOF). This solution model is selected based on the recommendations of the software documents [27]–[29]. The VOF model is used for bubbly and droplets flow patterns which occurring normally inside THP. In this model, each mesh cell considered to be occupied by the two phases together based on volume fraction of each phase. The mass transfer between the two phases and the other cells was calculated at each time interval of the solution. Also this model can truck the changes of both phases in transient and steady state processes. In this model, there is a single set of equations solved by iteration techniques for energy and momentum. Based on volume fractions (VF) of both phases in each cell, the appropriate thermal properties of each cell are calculated for momentum and energy calculations.

The following are the governing fluid flow, heat transfer/energy and two-phase mass transfer mathematical equations used to solve the 3DCFD model. These equations are used to solve the case study and get the transient and steady state parameters values and conditions of velocities, volume fractions (VF)of each phase and other thermal parameters [27]–[29]:

3.1. Continuity Equation

Due to heat supply at evaporation section and heat release at condenser section, the evaporation and condensation processes are kept continuous. Therefore, the VF of each phase keep change during operation of THP. For evaporation process and at each time interval, when a cell receive/absorb energy its temperature will raise. If the cell temperature exceeds evaporation temperature, a specific amount of liquid mass will evaporate based on the amount of absorbed energy and latent heat of evaporation h_{fg}. So that VOF of each phase will be calculated for the new time interval of calculations. Condensation occurs when the cell gave / release energy in opposite process of evaporation process.

Volume of fractions (VOF) values of the two-phases of the working fluid (water) are calculated one time at each time interval. The equation of continuity has the following form based on the coincide conservation of masses of both phases:

$$\nabla \cdot (\rho V) = -\frac{\partial \rho}{\partial t} \quad (1)$$

Equation (1) is initially solved to estimate the VF change of primary phase (v-vapor/ steam). Then eqn. (2) can track the VF change of the other phase (l-liquid/ condensate) as follow:

$$\nabla \cdot (\propto_l \rho_l V) = -\frac{\partial}{\partial t}(\propto_l \rho_l) + S_m \quad (2)$$

To estimate the mass transfer between the two phases during condensation and evaporation, a mass source (phase change) term S_m is added.

Equation (2) will not be solved for primary phase (vapor), because VF of vapor is calculated using the following expression:

$$\sum_{v=1}^{n} \propto_v = 1 \quad (3)$$

A mixture of the vapor (v) and liquid (l) phases exists when the cell is not wholly full with primary phase (v) or with the secondary phase (l). So that, the mixture density is calculated as the averaged density from volume fractions as follows:

$$\rho = \propto_l \rho_l + (1 - \propto_l)\rho_v \quad (4)$$

3.2. Momentum Equation

The main forces that effect on the momentum of the fluid phases in VOF model are friction, surface tension, gravitational, and pressure. Along the interface of the two phases, the effect of surface tension is important. So that a parameter named continuum surface force (F_{CSF}) has been added to the momentum equation:

$$F_{CSF} = 2\sigma \frac{\propto_l \rho_l C_v \nabla \alpha_v + \propto_v \rho_v C_l \nabla \alpha_l}{\rho_l + \rho_v} \quad (5)$$

When considering the effect of F_{CSF} forces into VOF model, the 3D momentum equation will be as follows:

$$\frac{\partial}{\partial t}(\rho V) + \nabla \cdot (\rho V V^T) = \rho g - \nabla p + \nabla \cdot \left[\mu(\nabla V + (\nabla V)^T) - \frac{2}{3}\mu(\nabla \cdot V) I\right] + F_{CSF} \quad (6)$$

The dynamic viscosity μ was considered mass averaged and calculated as follow:

$$\mu = \propto_l \mu_l + (1 - \propto_l)\mu_v \quad (7)$$

3.3. Energy Equation

In VOF model, there is a single set of equations for energy, and set as follows:

$$\frac{\partial}{\partial t}(\rho E) + \nabla \cdot (\rho E V) = \nabla \cdot (k \nabla \mathrm{T}) + \nabla \cdot (\mathrm{pV}) + S_E \quad (8)$$

To calculate the heat transfer during condensation and evaporation processes, an energy source parameter S_E is added.

The thermal conductivity k considered as mass averaged, and calculated as follows:

$$k = \propto_l k_l + (1 - \propto_l) k_v \quad (9)$$

Also energy E is considered as mass averaged, and calculated as follows:

$$E = \frac{\propto_l \rho_l E_l + \propto_v \rho_v E_v}{\propto_l \rho_l + \propto_v \rho_v} \quad (10)$$

Finally, for each phase, energy terms based on temperatures and specific heats are calculated as follows:

$$E_l = C_{v,l}(T - T_{sat}) \quad (11)$$

$$E_v = C_{v,v}(T - T_{sat}) \quad (12)$$

3.4. Thermal Resistance

There are different ways used to summarize the thermal performance of THP for validation purpose between different configurations. These different configurations could be working fluid, pipe material, size/geometry and filling ratio. The validation done for the same working parameters or boundary conditions (i.e. supplied heat , cooling system , inclination angle) [3][1](I. Saad et. al.,2017) [30]. The most favorable equation used for validation purpose is the thermal resistance equation [1], [31]–[33]:

$$R_{th} = \frac{T_{evap.avg.} - T_{cond.avg.}}{Q_{input}} \quad (13)$$

Therefore, the lower thermal resistance value for the THP is the better thermal performance among all suggested and tested configurations for the same boundary/operating conditions.

The enhancement percentage of the thermal performance is calculated from the reduction percentage for the R_{th} that calculated as follows:

$$\%\ Reduction\ of\ R_{th} = \frac{R_{th,normal} - R_{th,enhanced}}{R_{th,normal}} * 100 \quad (14)$$

4. Solution setup

The 3DCFD solution is done with ANSYS R 19.0 software and the solution setup are as in ref. [4], [26] according to the software documents recommendations [27]–[29]. The Volume of Fluid (VOF) solution model is set as a solution model for the fluid domain. The TP set as thermally Coupled walls to consider the heat transfer from/to the TP material during the solution calculations. The fluid adaptation technique is used to set up the FR with a transient time step of 10^{-4} Sec. The steady state conditions achieved when the supplied heat totally absorbed by the cooling water.

5. Results and Discussion

The resultant data from the 3DCFD solution are gathered for steady state conditions for the tested operating conditions. The steady state conditions are achieved when the supplied heat transferred totally to the cooling water during the operation. The results plotted as a velocity vectors at the central vertical plane of the TPTHP. This plot clarifies the effect of the insertion of TP on the velocity vectors of both phases as shown in fig. (7) for FR of 55% and supplied heat of 100W. All the tested operating configurations show the same behaviors for the velocity vectors due to the insertion of TP.

The velocity vectors show that the TPTHP has a very low rates/vanished of the spatial complex flow patterns formation. This low rates are with respect to the velocity vectors distribution of the THP that shown in fig. (2). The axial velocity vectors (along the TPTHP) are presented as the main flow velocity vectors. The cross velocity vectors are very low, and present mainly at the entrance/exit of the tubes. Therefore, the using/inserting of TP into the THP increases the uniformity of the distribution of velocity vectors. Also make the axial velocity vectors as the main vectors. Then the flow of both the generated steam and the condensate streams have been more regular without interactions during the evaporation/condensation processes. This regulation enhances and regulate the evaporation/ condensation cycle.

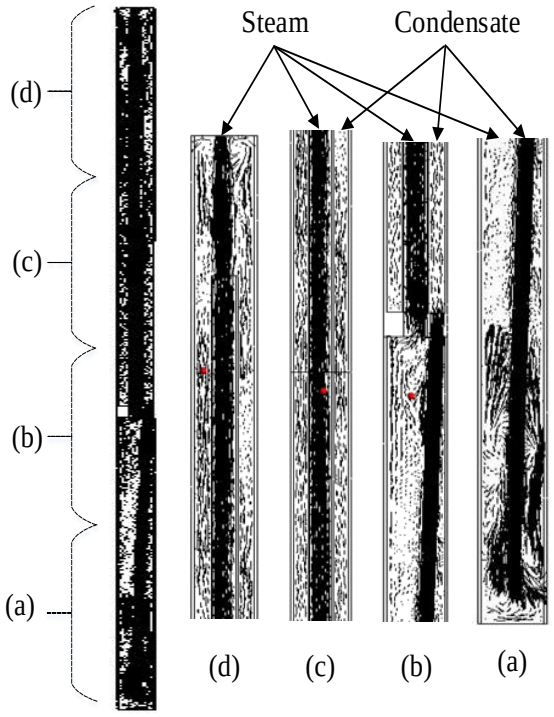

Figure 7. Velocity Vectors at Vertical Central Section of TPTHP

The Steam Volume Fractions (SVF) contours for the steady state operation of the THP and TPTHP are plotted at the central plane as shown in fig. (8). The TPTHP SVF contours clearly showed that the two phases streams are separated from each other. The generated steam streams flow upward through the riser tube to the upper portion of the condenser section. The condensate streams flow downward through the down comer tube to the lower portion of the evaporator section. The

interactions between the two streams are vanished. The spatial flow behavior is controlled and transformed to a regular circulation flow behavior. This new flow behavior inside the modified THP will leads to enhance the thermal performance of the THP.

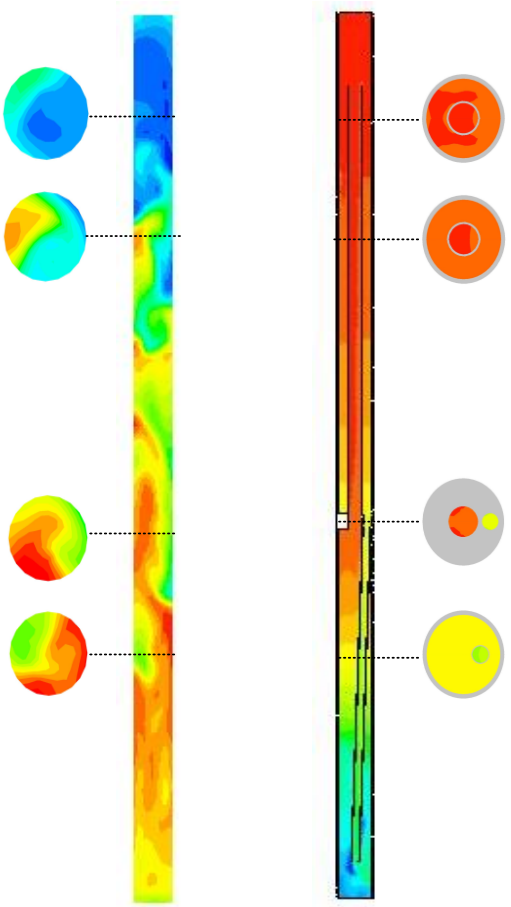

(a) THP (b) TPTHP

Figure 8. Steam Volume Fractions at the Central Vertical Plane of THP and TPTHP

The temperature distribution along the inner surface of the THP and TPTHP showed the same trend behaviors as shown in fig. (9, a-e). Along the evaporator section, it's clear that the TPTHP temperatures trends has a lower values of temperatures than that of the THP. Also the condenser section temperature distribution has a relatively higher values for the TPTHP than that of the THP. These lower trends for the evaporator section and higher trends for the condenser section represent the enhancement of the THP thermal performance due to the insertion of TP. The relatively lower values of temperatures along the evaporator section will produce a relatively lower values of the average temperatures of evaporator section. The relatively higher values of temperatures along the condenser section will produce a relatively higher values of the average temperatures of condenser section. Hence, according to eqn. (13) the TPTHP have a lower value of R_{th} Than THP. The decreasing of R_{th} values due to the insertion of TP represent the enhancement in the thermal performance.

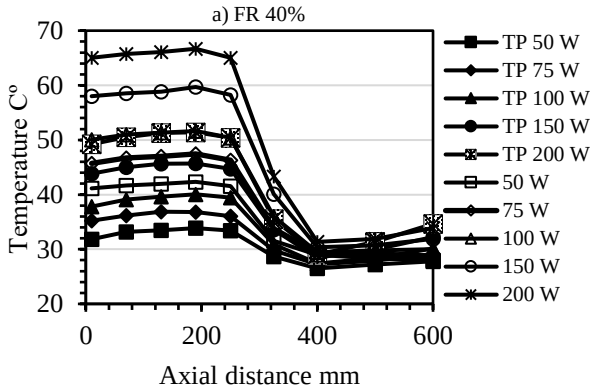

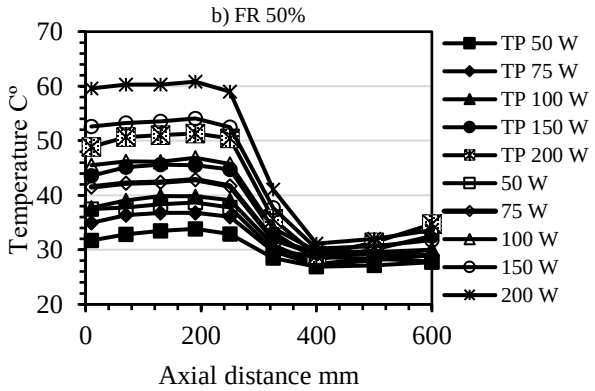

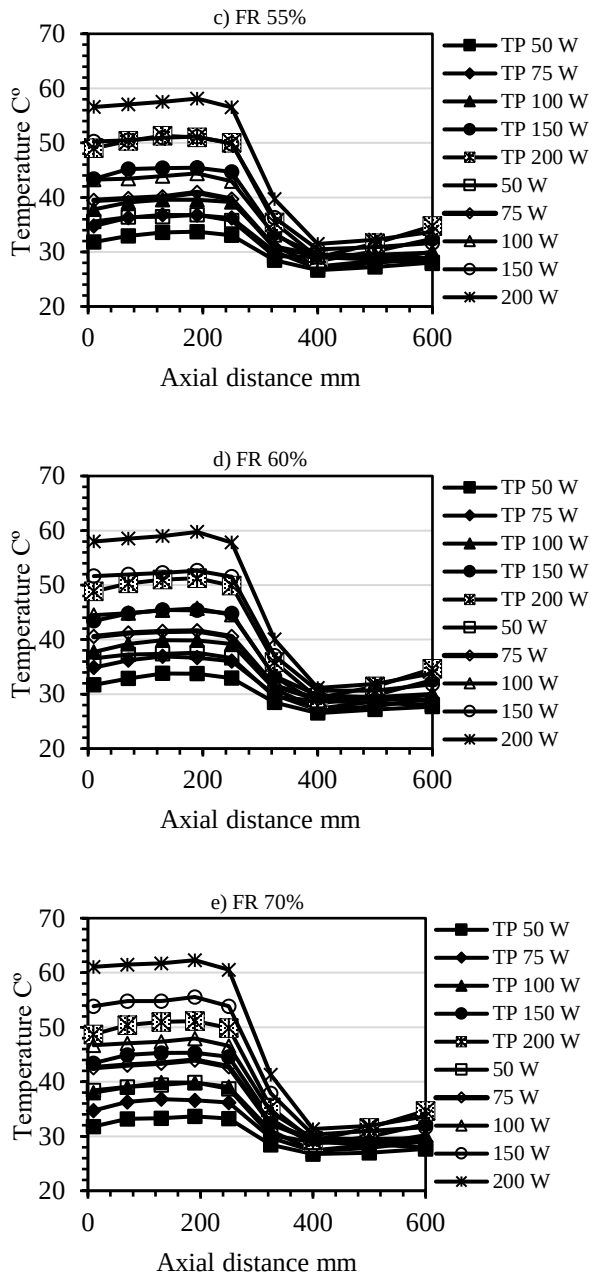

Figure (9, a-e) : Temperatures Distribution Along the THP and TPTHP

The effect of the insertion of TP on the values of R_{th} are shown in fig. (10). The trends for the TPTHP are clearly lower than the trends for the THP. Therefore, the insertion of the TP enhance/reduce the values of R_{th} and represent the enhancement of the thermal performance of the THP. The trends for the TPTHP are seemed to be coincided with each other for different values of FR rather than those for the THP that appears as a separated trends. These coincided trends for the TPTHP declare that the variation of FR does not affect the values of R_{th} at the same heat supply values. So that the insertion of the TP reduce/vanish the effect of the variations of FR on the thermal performance of the THP.

This result can be extrapolated to another results. The insertion of TP prevent/reduce the entrainment phenomenon effects. Entrainment phenomenon effects could lead to flooding situation and dropping of the thermal performance of the THP.

The trends show that the values of R_{th} are decreased when the supplied heat is increased. This behavior is related to the arrangement of eqn. (13). The maximum enhancement percentage gained due to the insertion of TP is the maximum reduction percentages of R_{th} value for the tested configurations. The maximum reduction percentages gained of R_{th} values is 55% for FR 40% and supplied heat of 50 W as showed in fig. (11).

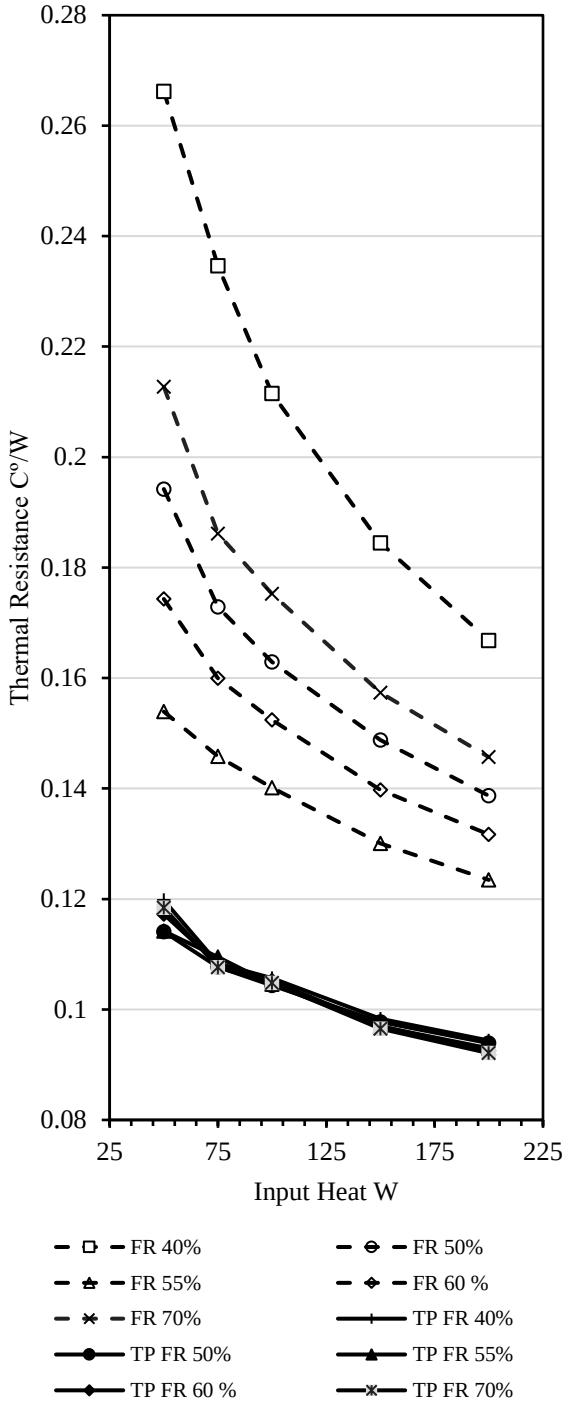

Figure 10. Effect of the Insertion of TP on Thermal Resistance of THP

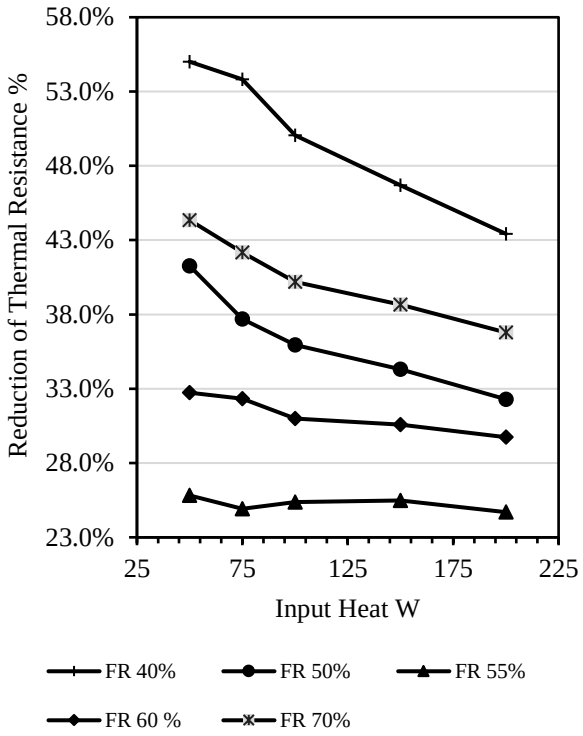

Figure 11. Reduction Percentages of R_{th} due to insertion of TP

6. Conclusions

A numerical study is carried out to simulate the flow fields for steam and condensate flow in THP. Simulation results showed a high interaction between the two phases.

Therefore, a new tubes packing is proposed on geometry basis to control the flow of the two-phases. This tubes packing is designed and tested in a 3DCFD simulation model. The simulation results showed that the flow paths facilitate the moving of the generated steam and the condensate streams. This facilitating leads to regulate/enhance the evaporation and condensation processes. Also this regulate produce a reduction of the thermal resistance of the THP up to 55% at various operating conditions. Hence the thermal performance of the THP are enhanced. The insertion of the TP reduce/vanish the effect of the variation of filling ratio on the thermal performance of the THP.

Acknowledgement

Authors wishing to acknowledge the Iraqi ministry of Electricity and Al-Mustansiriayah University / College of Engineering for supporting this research in all its steps.

Abbreviations

FR	Filling Ratio
HP	Heat Pipe
PCM	Phase Change Material
SVF	Steam Volume Fraction
VF	Volume Fraction
VOF	Volume Of Fluid
THP	Thermosyphon Heat Pipe
TP	Tubes Packing
TPTHP	Thermosyphon Heat Pipe with Tubes Packing

Nomenclature

A	Area	m^2
C	Coefficient of surface curvature	(-)
$C_{v,l}$	Specific heat	kJ/kg K
d	Diameter	m
E	Energy	kJ
g	Gravitational acceleration	m/sec^2
h	Convection heat transfer coefficient	W/ m.K
I	Unit tensor	
k	Thermal conductivity	W/ m^2.K
l	Length	m
m	Mass	kg
n	Number of data points	
p	Pressure	pa
Q	Supplied heat	W
R_{th}	Thermal resistance	K/W
S_E	Energy source parameter	kJ
S_m	Phase change (mass source)	
T	Temperature	K
t	Time	Sec
t	Thickness	m
$T_{evap.avg.}$	Average temperature of evaporator section	K
$T_{cond.avg.}$	Average temperature of condenser section	K
V	Velocity vector	
V	Volume	m^3
v	Velocity	m/sec
v	Specific volume	m^3/kg
x	Dryness fraction	[---]
α_l	Liquid volume fraction	(-)
α_v	Vapor volume fraction	(-)
μ	Dynamic viscosity	N sec/m^2
ρ	Density	kg/m^3
σ	Surface tension	N/m

Conflict of interest

There are not conflicts to declare.

7. References

1- D. A. Reay, P. A. Kew, and R. J. McGlen, (2014) *Heat pipes Theory, Design and Applications*, Sixth., no. 1. Elsevier,.

2- B. Zohuri, (2010) *Heat Pipe Design and Technology*. Taylor & Francis Group,.

3- M. Salem, (2017) *"A Review : on the Heat Pipe and Its Applications,"* in *4th International Conference on Energy Engineering*, , no. December.

4- A. A. B. Temimy and A. A. Abdulrasool, (2019) *"CFD Modelling for flow and heat transfer in a closed Thermosyphon charged with water – A new observation for the two phase interaction,"* in *Second International Conference on Sustainable Engineering Techniques*,.

5- S. Föste, F. Giovannetti, S. Jack, B. Schiebler, and G. Rockendorf, (2015) *"Heat Pipe Collectors for Cost Reduction of Solar Installations,"* in *international Solar Energy Society*, 2015, no. July, pp. 1–10.

6- S. Aswath, V. H. Netaji Naidu, P. Padmanathan, and Y. Raja Sekhar, (2017) *"Multiphase numerical analysis of heat*

pipe with different working fluids for solar applications," IOP Conf. Ser. Mater. Sci. Eng., vol. 263, no. 6, pp. 0–6,.

7- K. Zhu, X. Li, Y. Wang, X. Chen, and H. Li, (2017) *"Dynamic performance of loop heat pipes for cooling of electronics," Energy Procedia*, vol. 142, no. February 2018, pp. 4163–4168,.

8- M. Smitka, Z. Kolková, P. Nemec, and M. Malcho, (2014) *"Impact of the amount of working fluid in loop heat pipe to remove waste heat from electronic component," EPJ Web Conf.*, vol. 67, p. 02109,.

9- N. S. Chougule, T. S. Jadhav, and M. M. Lele, (2016) *"A Review on Heat Pipe for Air Conditioning applications," Int. J. Curr. Eng. Technol.*, no. April,.

10- R. R. Riehl, *"Heat pipes and loop heat pipes acceptance tests for satellites applications, (2020)* " *AIP Conf. Proc.*, vol. 1103, no. March 2009, pp. 82–90, 2009.

11- P. M. Dussinger, B. S. David, and W. G. Anderson, (2009) *"Loop heat pipe for TacSat-4," AIP Conf. Proc.*, vol. 1103, no. March, pp. 91–100,.

12- M. Rahimi, K. Asgary, and S. Jesri, (2010) *"Thermal characteristics of a resurfaced condenser and evaporator closed two-phase thermosyphon," Int. Commun. Heat Mass Transf.*, vol. 37, no. 6, pp. 703–710,.

13- T. Israeli, T. A. Reddy, and Y. I. Cho, (2008) *"Investigation on the Use of Nanofluids to Enhance Heat Pipe Performance,"* in *international Solar Energy Conference*, , no. January, pp. 243–251.

14- S. Zhao, G. Xu, N. Wang, and Z. Zhang, (2018) *"Experimental Study on the Thermal Start-Up Performance of the Graphene/Water Nanofluid-Enhanced Solar Gravity Heat Pipe," Nanomaterials*, vol. 8, no. 2, p. 72,.

15- K. M. Armijo and V. P. Carey, (2011) *"An Experimental Study of Heat Pipe Performance Using Binary Mixture Fluids That Exhibit Strong Concentration* Marangoni Effects," *J. Therm. Sci. Eng. Appl.*, vol. 3, no. 3, p. 031003,.

16- Y. Naresh, K. Shri Vignesh, and C. Balaji, (2018) *"Experimental investigations of the thermal performance of self-rewetting fluids in internally finned wickless heat pipes," Exp. Therm. Fluid Sci.*, vol. 92, pp. 436–446,.

17- Y. C. Weng, H. P. Cho, C. C. Chang, and S. L. Chen, (2011) *"Heat pipe with PCM for electronic cooling," Appl. Energy*, vol. 88, no. 5, pp. 1825–1833,.

18- H. Behi, M. Ghanbarpour, and M. Behi, (2017) *"Investigation of PCM-assisted heat pipe for electronic cooling," Appl. Therm. Eng.*, vol. 127, pp. 1132–1142,.

19- H. Hashimoto and F. Kaminaga, *"Heat transfer characteristics in a condenser of closed two-phase thermosyphon: Effect of entrainment on heat transfer deterioration 2002," Heat Transf. - Asian Res.*, vol. 31, no. 3, pp. 212–225,.

20- Y. M. Hung and Q. Seng, (2011) *"Effects of geometric design on thermal performance of star-groove micro-heat pipes," Int. J. Heat Mass Transf.*, vol. 54, no. 5–6, pp. 1198–1209,.

21- R. Nair and C. Balaji, (2016) "Synergistic analysis of heat transfer characteristics of an internally finned two phase closed thermosyphon," *Appl. Therm. Eng.*, vol. 101, pp. 720–729,.

22- A. Brusly Solomon *et al.*, (2017) *"Performance enhancement of a two-phase closed thermosiphon with a thin porous copper coating," Int. Commun. Heat Mass Transf.*, vol. 82, pp. 9–19,.

23- S. E. D. Fertahi, T. Bouhal, Y. Agrouaz, T. Kousksou, T. El Rhafiki, and Y.

Zeraouli, (2018) *"Performance optimization of a two-phase closed thermosyphon through CFD numerical simulations," Appl. Therm. Eng.*, vol. 128, pp. 551–563,.

24- A. A. Alammar, F. N. Al-Mousawi, R. K. Al-Dadah, S. M. Mahmoud, and R. Hood, (2018) *"Enhancing thermal performance of a two-phase closed thermosyphon with an internal surface roughness*," *J. Clean. Prod.*, vol. 185, pp. 128–136,.

25- Y. Kim, D. H. Shin, J. S. Kim, S. M. You, and J. Lee, (2019) *"Effect of sintered microporous coating at the evaporator on the thermal performance of a two-phase closed thermosyphon," Int. J. Heat Mass Transf.*, vol. 131, pp. 1064–1074,.

26- A. A. B. Temimy and A. A. Abdulrasool, (2019) *"Numerical Modelling and Experimental Verification of New Observations of the Two Phases Interaction in a Vertical and Inclined Closed Wickless Heat Pipe," J. Univ. Babylon Eng. Sci.*, vol. 27, no. 3,.

27- T. D. Canonsburg, *ANSYS FLUENT Theory Guide*. 2018.

28- T. D. Canonsburg, *ANSYS FLUENT Tutorial Guide*. 2018.

29- T. D. Canonsburg, *ANSYS FLUENT User ' s Guide*. 2018.

30- I. Saad *et al.*, (2017) *"Heat pipe based systems - Advances and applications," Energy*, vol. 128, pp. 729–754,.

31- S. Lips, V. Sartre, F. Lefèvre, S. Khandekar, and J. Bonjour, (2017) *"Overview of heat pipe studies during the period 2010-2015,".*

32- L. Id, *"Heat Pipe Principles*(1988*)" Int. J. Heat Mass Transf.*, vol. 3, pp. 112–125,.

33- Frank P. Incropera, David P. DeWitt, Theodore L. Bergman, and Adrienne S. Lavine, *Fundamentals of Heat and Mass Transfer*, Sixth. John Wiley & Sons, 2006.